

4. Electron Dynamics in Solids

In the previous chapter we have seen how the single-electron energy states form a band structure in the presence of a lattice. Our goal now is to understand the consequences of this, so that we can start to get a feel for some of the basic properties of materials.

There is one feature in particular that will be important: materials don't just have one electron sitting in them. They have lots. A large part of condensed matter physics is concerned with understanding the collective behaviour of this swarm of electrons. This can often involve the interactions between electrons giving rise to subtle and surprising effects. However, for our initial foray into this problem, we will make a fairly brutal simplification: we will ignore the interactions between electrons. Ultimately, much of the basic physics that we describe below is unchanged if we turn on interactions, although the reason for this turns out to be rather deep.

4.1 Fermi Surfaces

Even in the absence of any interactions, electrons still are still affected by the presence of others. This is because electrons are fermions, and so subject to the *Pauli exclusion principle*. This is the statement that only one electron can sit in any given state. As we will see below, the Pauli exclusion principle, coupled with the general features of band structure, goes some way towards explaining the main properties of materials.

Free Electrons

As a simple example, suppose that we have no lattice. We take a cubic box, with sides of length L , and throw in some large number of electrons. What is the lowest energy state of this system? Free electrons sit in eigenstates with momentum $\hbar\mathbf{k}$ and energy $E = \hbar^2 k^2 / 2m$. Because we have a system of finite size, momenta are quantised as $k_i = 2\pi n_i / L$. Further, they also carry one of two spin states, $|\uparrow\rangle$ or $|\downarrow\rangle$.

The first electron can sit in the state $\mathbf{k} = 0$ with, say, spin $|\uparrow\rangle$. The second electron can also have $\mathbf{k} = 0$, but must have spin $|\downarrow\rangle$, opposite to the first. Neither of these electrons costs any energy. However, the next electron is not so lucky. The minimum energy state it can sit in has $n_i = (1, 0, 0)$. Including spin and momentum there are a total of six electrons which can carry momentum $|\mathbf{k}| = 2\pi/L$. As we go on, we fill out a ball in momentum space. This ball is called the *Fermi sea* and the boundary of the ball is called the *Fermi surface*. The states on the Fermi surface are said to have

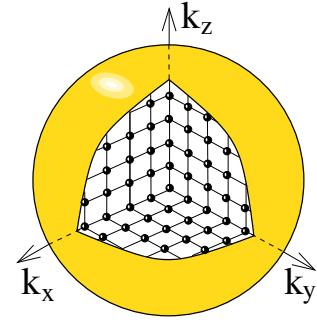


Figure 52: The Fermi surface

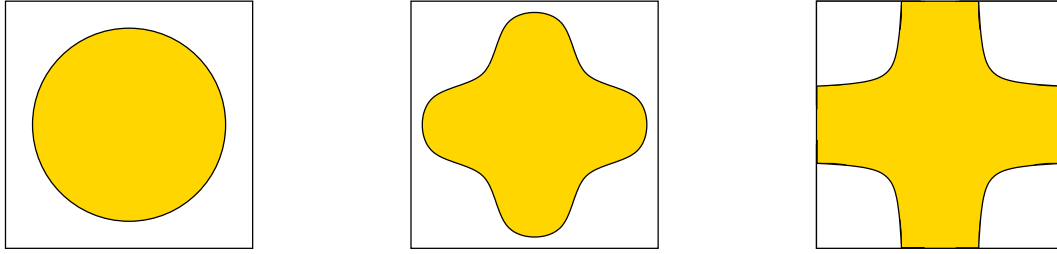


Figure 53: Fermi surfaces for valence $Z = 1$ with increasing lattice strength.

Fermi momentum $\hbar k_F$ and *Fermi energy* $E_F = \hbar^2 k_F^2 / 2m$. Various properties of the free Fermi sea are explored in the lectures on [Statistical Physics](#).

4.1.1 Metals vs Insulators

Here we would like to understand what becomes of the Fermi sea and, more importantly, the Fermi surface in the presence of a lattice. Let's recapitulate some important facts that we'll need to proceed:

- A lattice causes the energy spectrum to split into bands. We saw in Section [3.3.2](#) that a Bravais lattice with N sites results in each band having N momentum states. These are either labelled by momenta in the first Brillouin zone (in the reduced zone scheme) or by momentum in successive Brillouin zones (in the extended zone scheme).
- Because each electron carries one of two spin states, each band can accommodate $2N$ electrons.
- Each atom of the lattice provides an integer number of electrons, Z , which are free to roam the material. These are called *valence electrons* and the atom is said to have *valence* Z .

From this, we can piece the rest of the story together. We'll discuss the situation for two-dimensional square lattices because it's simple to draw the Brillouin zones. But everything we say carries over for more complicated lattices in three-dimensions.

Suppose that our atoms have valence $Z = 1$. There are then N electrons, which can be comfortably housed inside the first Brillouin zone. In the left-hand of Figure [53](#) we have drawn the Fermi surface for free electrons inside the first Brillouin zone. However, we know that the effect of the lattice is to reduce the energy at the edges of the Brillouin zone. We expect, therefore, that the Fermi surface — which is the

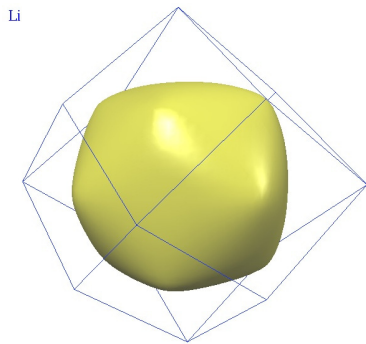


Figure 54: Lithium.

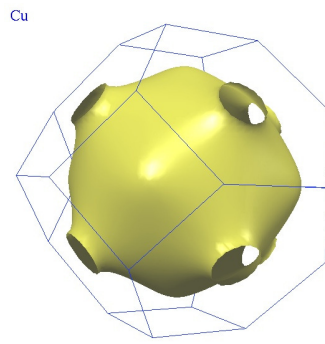


Figure 55: Copper.

equipotential E_F — will be distorted as shown in the middle figure, with states closer to the edge of the Brillouin zone filled preferentially. Note that the area inside the Fermi surface remains the same.

If the effects of the lattice get very strong, it may be that the Fermi surface touches the edge of the Brillouin zone as shown in the right-hand drawing in Figure 53. Because the Brillouin zone is a torus, if the Fermi surface is to be smooth then it must hit the edge of the Brillouin zone at right-angles.

This same physics can be seen in real Fermi surfaces. Lithium has valence $Z = 1$. It forms a BCC lattice, and so the Brillouin zone is FCC. Its Fermi surface is shown above, plotted within its Brillouin zone⁶. Copper also has valency $Z = 1$, with a FCC lattice and hence BCC Brillouin zone. Here the effects of the lattice are somewhat stronger, and the Fermi surface touches the Brillouin zone.

In all of these cases, there are unoccupied states with arbitrarily small energy above E_F . (Strictly speaking, this statement holds only in the limit $L \rightarrow \infty$ of an infinitely large lattice.) This means that if we perturb the system in any way, the electrons will easily be able to respond. Note, however, that only those electrons close to the Fermi surface can respond; those that lie deep within the Fermi sea are locked there by the Pauli exclusion principle and require much larger amounts of energy if they wish to escape.

This is an important point, so I'll say it again. In most situations, only those electrons which lie on the Fermi surface can actually do anything. This is why Fermi surfaces play such a crucial role in our understanding of materials.

⁶This, and other pictures of Fermi surfaces, are taken from <http://www.phys.ufl.edu/fermisurface/>.

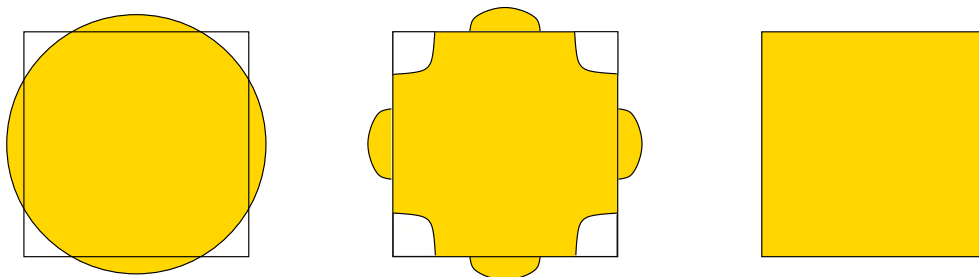


Figure 56: Fermi surfaces for valence $Z = 2$ with increasing lattice strength, moving from a metal to an insulator.

Materials with a Fermi surface are called *metals*. Suppose, for example, that we apply a small electric field to the sample. The electrons that lie at the Fermi surface can move to different available states in order to minimize their energy in the presence of the electric field. This results in a current that flows, the key characteristic of a metal. We'll discuss more about how electrons in lattices respond to outside influences in Section 4.2

Before we move on, a couple of comments:

- The Fermi energy of metals is huge, corresponding to a temperature of $E_F/k_B \sim 10^4 K$, much higher than the melting temperature. For this reason, the zero temperature analysis is a good starting point for thinking about real materials.
- Metals have a very large number of low-energy excitations, proportional to the area of the Fermi surface. This makes metals a particularly interesting theoretical challenge.

Let's now consider atoms with valency $Z = 2$. These have $2N$ mobile electrons, exactly the right number to fill the first band. However, in the free electron picture, this is not what happens. Instead, they partially fill the first Brillouin zone and then spill over into the second Brillouin zone. The resulting Fermi surface, drawn in the extended zone scheme, is shown in left-hand picture of Figure 56

If the effects of the lattice are weak, this will not be greatly changed. Both the first and second Brillouin zones will have available states close to the Fermi surface as shown in the middle picture. These materials remain metals. We sometimes talk

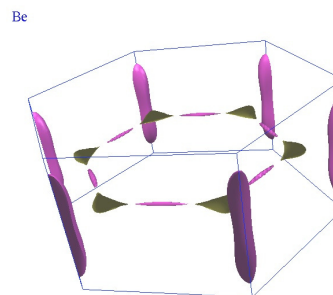


Figure 57: Beryllium

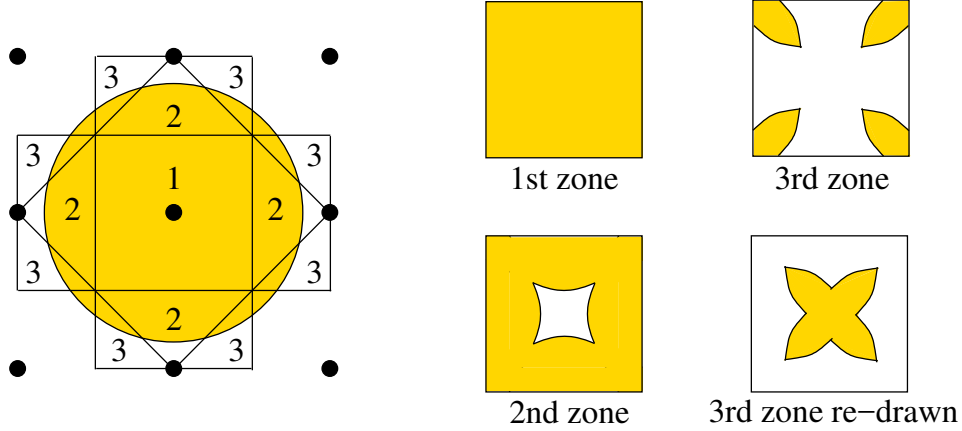


Figure 58: Fermi surfaces for valence $Z = 3$.

of electrons in the second band, and holes (i.e. absence of electrons) in the first band. We will discuss this further in Section 4.2. Beryllium provides an example of a metal with $Z = 2$; its Fermi surface is shown in the figure, now plotted in the reduced zone scheme. It includes both an electron Fermi surface (the cigar-like shapes around the edge) and a hole Fermi surface (the crown in the middle).

Finally, if the effects of the lattice become very strong, the gap between the two bands is large enough to overcome the original difference in kinetic energies. This occurs when the lowest lying state in the second band is higher than the highest state in the first. Now the electrons fill the first band. The second band is empty. The Fermi sea looks like the right-hand picture in Figure 56. This is qualitatively different from previous situations. There is no Fermi surface and, correspondingly, no low-energy excitations. Any electron that wishes to change its state can only do so by jumping to the next band. But that costs a finite amount of energy, equal to the gap between bands. This means that all the electrons are now locked in place and cannot respond to arbitrarily small outside influences. We call such materials *insulators*. (Sometimes they are referred to as *band insulators* to highlight the fact that it is the band structure which prevents the electrons from moving.)

This basic characterisation remains for higher valency Z . Systems with partially filled bands are metals; systems with only fully-filled bands are insulators. Note that a metal may well have several fully-filled bands, before we get to a partially filled band. In such circumstances, we usually differentiate between the fully-filled lower bands — which are called *valence bands* — and the partially filled *conduction band*.

The Fermi surfaces may exist in several different bands. An example of a Fermi surface for $Z = 3$ is shown in Figure 58, the first three Brillouin zones are shown separately in the reduced zone scheme. At first glance, it appears that the Fermi surface in the 3rd Brillouin zone is disconnected. However, we have to remember that the edges of the Brillouin zone are identified. Re-drawn, with the origin taken to be $\mathbf{k} = (\pi/a, \pi/a)$, we see the Fermi surface is connected, taking the rosette shape shown.

Looking Forwards

We have seen how band structure allows us to classify all materials as metals or insulators. This, however, is just the beginning, the first chapter in a long and detailed story which extends from physics into materials science. To whet the appetite, here are three twists that we can add to this basic classification.

- For insulators, the energy required to reach the first excited state is set by the band gap Δ which, in turn, is determined by microscopic considerations. Materials whose band gap is smaller than $\Delta \lesssim 2 \text{ eV}$ or so behave as insulators at small temperature, but starts to conduct at higher temperatures as electrons are thermally excited from the valence band to the conduction band. Such materials are called *semiconductors*. They have the property that their conductivity increases as the temperature increases. (This is in contrast to metals whose conductivity decreases as temperature increases.) John Bardeen, Walter Brattain and William Shockley won the 1956 Nobel prize for developing their understanding of semiconductors into a working transistor. This, then, changed the world.
- There are some materials which have $Z = 1$ but are, nonetheless, insulators. An example is nickel oxide NiO . This contradicts our predictions using elementary band structure. The reason is that, for these materials, we cannot ignore the interactions between electrons. Roughly speaking, the repulsive force dominates the physics and effectively prohibits two electrons from sitting on the same site, even if they have different spins. But with only one spin state allowed per site, each band houses only N electrons. Materials with this property are referred to as *Mott insulators*. Nevill Mott, Cavendish professor and master of Caius, won the 1977 Nobel prize, in part for this discovery.
- For a long time band insulators were considered boring. The gap to the first excited state means that they can't do anything when prodded gently. This attitude changed relatively recently when it was realised that you can be boring in different ways. There is a topological classification of how the phase of the quantum states winds as you move around the Brillouin zone. Materials in which

this winding is non-trivial are called *topological insulators*. They have wonderful and surprising properties, most notably on their edges where they come alive with interesting and novel physics. David Thouless and Duncan Haldane won the 2016 Nobel prize for their early, pioneering work on this topic.

More generally, there is a lesson above that holds in a much wider context. Our classification of materials into metals and insulators hinges on whether or not we can excite a multi-electron system with an arbitrarily small cost in energy. For insulators, this is not possible: we require a finite injection of energy to reach the excited states. Such systems are referred to as *gapped*, meaning that there is finite energy gap between the ground state and first excited state. Meanwhile, systems like metals are called *gapless*. Deciding whether any given quantum system is gapped or gapless is one of the most basic questions we can ask. It can also be one of the hardest. For example, the question of whether a quantum system known as *Yang-Mills theory* has a gap is one of the six unsolved millenium maths problems.

4.1.2 The Discovery of Band Structure

Much of the basic theory of band structure was laid down by Felix Bloch in 1928 as part of his doctoral thesis. As we have seen, Bloch's name is attached to large swathes of the subject. He had an extremely successful career, winning the Nobel prize in 1952, working as the first director-general of CERN, and building the fledgling physics department at Stanford University.

However, Bloch missed the key insight that band structure explains the difference between metals and insulators. This was made by Alan Wilson, a name less well known to physicists. Wilson was a student of Ralph Fowler in Cambridge. In 1931, he took up a research position with Heisenberg and it was here that he made his important breakthrough. He returned on a visit to Cambridge to spread the joy of his newfound discovery, only to find that no one very much cared. At the time, Cambridge was in the thrall of Rutherford and his motto: "There are two kinds of science, physics and stamp collecting". And when Rutherford said "physics", he meant "nuclear physics".

This, from Nevill Mott,

"I first heard of [Wilson's discovery] when Fowler was explaining it to Charles Ellis, one of Rutherford's closest collaborators, who said 'very interesting' in a tone which implied that he was not interested at all. Neither was I."

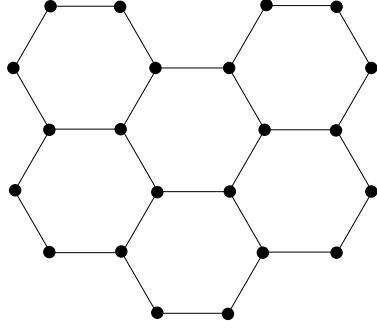


Figure 59: The honeycomb lattice.

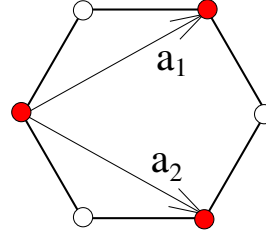


Figure 60: And its basis vectors.

Nevill Mott went on to win the Nobel prize for generalising Wilson’s ideas. Wilson himself didn’t do so badly either. He left academia and moved to industry, rising to become chairman of Glaxo.

4.1.3 Graphene

Graphene is a two-dimensional lattice of carbon atoms, arranged in a honeycomb structure as shown in the figure. Although it is straightforward to build many layers of these lattices — a substance known as graphite — it was long thought that a purely two-dimensional lattice would be unstable to thermal fluctuations and impossible to create. This changed in 2004 when Andre Geim and Konstantin Novoselov at the University of Manchester succeeded in isolating two-dimensional graphene. For this, they won the 2010 Nobel prize. As we now show, the band structure of graphene is particularly interesting.

First, some basic lattice facts. We described the honeycomb lattice in Section 3.2.1. It is not Bravais. Instead, it is best thought of as two triangular sublattices. We define the primitive lattice vectors

$$\mathbf{a}_1 = \frac{\sqrt{3}a}{2}(\sqrt{3}, 1) \quad \text{and} \quad \mathbf{a}_2 = \frac{\sqrt{3}a}{2}(\sqrt{3}, -1)$$

where a the distance between neighbouring atoms, which in graphene is about $a \approx 1.4 \times 10^{-10} \text{ m}$. These lattice vectors are shown in the figure.

Sublattice A is defined as all the points $\mathbf{r} = n_1\mathbf{a}_1 + n_2\mathbf{a}_2$ with $n_i \in \mathbf{Z}$. These are the red dots in the figure. Sublattice B is defined as all points $\mathbf{r} = n_1\mathbf{a}_1 + n_2\mathbf{a}_2 + \mathbf{d}$ with $\mathbf{d} = (-a, 0)$. These are the white dots.

The reciprocal lattice is generated by vectors \mathbf{b}_j satisfying $\mathbf{a}_i \cdot \mathbf{b}_j = 2\pi\delta_{ij}$. These are

$$\mathbf{b}_1 = \frac{2\pi}{3a}(1, \sqrt{3}) \quad \text{and} \quad \mathbf{b}_2 = \frac{2\pi}{3a}(1, -\sqrt{3})$$

This reciprocal lattice is also triangular, rotated 90° from the original. The Brillouin zone is constructed in the usual manner by drawing perpendicular boundaries between the origin and each other point in the reciprocal lattice. This is shown in the figure. We shortly see that the corners of the Brillouin zone carry particular interest. It naively appears that there are 6 corners, but this should really be viewed as two sets of three. This follows because any points in the Brillouin zone which are connected by a reciprocal lattice vector are identified. Representatives of the two, inequivalent corners of the Brillouin zone are given by

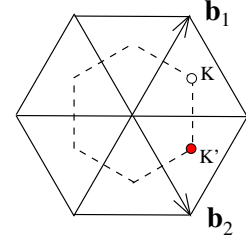


Figure 61:

$$\mathbf{K} = \frac{1}{3}(2\mathbf{b}_1 + \mathbf{b}_2) = \frac{2\pi}{3a} \left(1, \frac{1}{\sqrt{3}}\right) \quad \text{and} \quad \mathbf{K}' = \frac{1}{3}(\mathbf{b}_1 + 2\mathbf{b}_2) = \frac{2\pi}{3a} \left(1, -\frac{1}{\sqrt{3}}\right) \quad (4.1)$$

These are shown in the figure above.

Tight Binding for Graphene

The carbon atoms in graphene have valency $Z = 1$, with the p_z -atomic orbital abandoned by their parent ions and free to roam the lattice. In this context, it is usually called the π -orbital. We therefore write down a tight-binding model in which this electron can hop from one atomic site to another. We will work only with nearest neighbour interactions which, for the honeycomb lattice, means that the Hamiltonian admits hopping from a site of the A-lattice to the three nearest neighbours on the B-lattice, and vice versa. The Hamiltonian is given by

$$H = -t \sum_{\mathbf{r} \in \Lambda} \left[|\mathbf{r}; A\rangle \langle \mathbf{r}; B| + |\mathbf{r}; A\rangle \langle \mathbf{r} + \mathbf{a}_1; B| + |\mathbf{r}; A\rangle \langle \mathbf{r} + \mathbf{a}_2; B| + \text{h.c.} \right] \quad (4.2)$$

where we're using the notation

$$|\mathbf{r}; A\rangle = |\mathbf{r}\rangle \quad \text{and} \quad |\mathbf{r}; B\rangle = |\mathbf{r} + \mathbf{d}\rangle \quad \text{with} \quad \mathbf{d} = (-a, 0)$$

Comparing to (3.34), we have set $E_0 = 0$, on the grounds that it doesn't change any of the physics. For what it's worth, $t \approx 2.8 \text{ eV}$ in graphene, although we won't need the precise value to get at the key physics.

The energy eigenstates are again plane waves, but now with a suitable mixture of A and B sublattices. We make the ansatz

$$|\psi(\mathbf{k})\rangle = \frac{1}{\sqrt{2N}} \sum_{\mathbf{r} \in \Lambda} e^{i\mathbf{k} \cdot \mathbf{r}} \left(c_A |\mathbf{r}; A\rangle + c_B |\mathbf{r}; B\rangle \right)$$

Plugging this into the Schrödinger equation, we find that c_A and c_B must satisfy the eigenvalue equation

$$\begin{pmatrix} 0 & \gamma(\mathbf{k}) \\ \gamma^*(\mathbf{k}) & 0 \end{pmatrix} \begin{pmatrix} c_A \\ c_B \end{pmatrix} = E(\mathbf{k}) \begin{pmatrix} c_A \\ c_B \end{pmatrix} \quad (4.3)$$

where

$$\gamma(\mathbf{k}) = -t \left(1 + e^{i\mathbf{k} \cdot \mathbf{a}_1} + e^{i\mathbf{k} \cdot \mathbf{a}_2} \right)$$

The energy eigenvalues of (4.3) are simply

$$E(\mathbf{k}) = \pm |\gamma(\mathbf{k})|$$

We can write this as

$$E(\mathbf{k})^2 = t^2 \left| 1 + e^{i\mathbf{k} \cdot \mathbf{a}_1} + e^{i\mathbf{k} \cdot \mathbf{a}_2} \right|^2 = t^2 \left| 1 + 2e^{3ik_x a/2} \cos \left(\frac{\sqrt{3}k_y a}{2} \right) \right|^2$$

Expanding this out, we get the energy eigenvalues

$$E(\mathbf{k}) = \pm t \sqrt{1 + 4 \cos \left(\frac{3k_x a}{2} \right) \cos \left(\frac{\sqrt{3}k_y a}{2} \right) + 4 \cos^2 \left(\frac{\sqrt{3}k_y a}{2} \right)}$$

Note that the energy spectrum is a double cover of the first Brillouin zone, symmetric about $E = 0$. This doubling can be traced to the fact the the honeycomb lattice consists of two intertwined Bravais lattices. Because the carbon atoms have valency $Z = 1$, only the lower band with $E(\mathbf{k}) < 0$ will be filled.

The surprise of graphene is that these two bands meet at special points. These occur on the corners $\mathbf{k} = \mathbf{K}$ and $\mathbf{k} = \mathbf{K}'$ (4.1), where $\cos(3k_x a/2) = -1$ and $\cos(\sqrt{3}k_y a/2) = 1/2$. The resulting band structure is shown in Figure 62⁷. Because the lower band is filled, the Fermi surface in graphene consists of just two points, \mathbf{K} and \mathbf{K}' where the bands meet. It is an example of a *semi-metal*.

Emergent Relativistic Physics

The points $\mathbf{k} = \mathbf{K}$ and \mathbf{K}' where the bands meet are known as *Dirac points*. To see why, we linearise about these points. Write

$$\mathbf{k} = \mathbf{K} + \mathbf{q}$$

⁷The image is taken from the [exciting-code website](#).

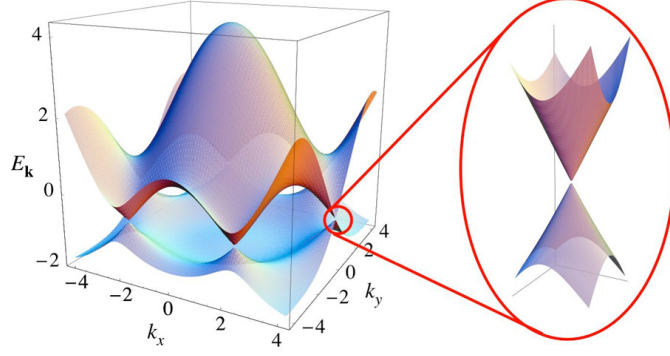


Figure 62: The band structure of graphene.

A little Taylor expansion shows that in the vicinity of the Dirac points, the dispersion relation is linear

$$E(\mathbf{k}) \approx \pm \frac{3ta}{2} |\mathbf{q}|$$

But this is the same kind of energy-momentum relation that we meet in relativistic physics for massless particles! In that case, we have $E = |\mathbf{p}|c$ where p is the momentum and c is the speed of light. For graphene, we have

$$E(\mathbf{k}) \approx \hbar v_F |\mathbf{q}|$$

where $\hbar \mathbf{q}$ is the momentum measured with respect to the Dirac point and $v_F = 3ta/2\hbar$ is the speed at which the excitations propagate. In graphene, v_F is about 300 times smaller than the speed of light. Nonetheless, it remains true that the low-energy excitations of graphene are governed by the same equations that we meet in relativistic quantum field theory. This was part of the reason for the excitement about graphene: we get to test ideas from quantum field theory in a simple desktop experiment.

We can tease out more of the relativistic structure by returning to the Hamiltonian (4.2). Close to the Dirac point $\mathbf{k} = \mathbf{K}$ we have

$$\begin{aligned} \gamma(\mathbf{k}) &= -t \left(1 - 2e^{3iq_x a/2} \cos \left(\frac{\pi}{3} + \frac{\sqrt{3}q_y a}{2} \right) \right) \\ &= -t \left(1 - 2e^{3iq_x a/2} \left[\frac{1}{2} \cos \left(\frac{\sqrt{3}q_y a}{2} \right) - \frac{\sqrt{3}}{2} \sin \left(\frac{\sqrt{3}q_y a}{2} \right) \right] \right) \\ &\approx -t \left(1 - 2 \left(1 + \frac{3iq_x a}{2} + \dots \right) \left(\frac{1}{2} - \frac{3q_y a}{4} + \dots \right) \right) \\ &\approx v_F \hbar (iq_x - q_y) \end{aligned}$$

This means that the Hamiltonian in the vicinity of the Dirac point $\mathbf{k} = \mathbf{K}$ takes the form

$$H = v_F \hbar \begin{pmatrix} 0 & iq_x - q_y \\ -iq_x - q_y & 0 \end{pmatrix} = -v_F \hbar (q_x \sigma^y + q_y \sigma^x) \quad (4.4)$$

where σ^x and σ^y are the Pauli matrices. But this is the *Dirac equation* for a massless particle moving in two-dimensions, sometimes referred to as the *Pauli equation*. (Note: our original choice of orientation of the honeycomb lattice has resulted in a slightly annoying expression for the Hamiltonian. Had we rotated by 90° to begin with, we would be left with the nicer $H = \hbar v_F \mathbf{q} \cdot \boldsymbol{\sigma}$ where $\boldsymbol{\sigma} = (\sigma^x, \sigma^y)$.)

There's something of an irony here. In the original Dirac equation, the 2×2 matrix structure comes about because the electron carries spin. But that's not the origin of the matrix structure in (4.4). Indeed, we've not mentioned spin anywhere in our discussion. Instead, in graphene the emergent "spin" degree of freedom arises from the existence of the two A and B sublattices.

We get a very similar equation in the vicinity of the other Dirac point. Expanding $\mathbf{k} = \mathbf{K}' + \mathbf{q}'$, we get the resulting Hamiltonian

$$H = -v_F \hbar (q_x \sigma^y - q_y \sigma^x)$$

The difference in minus sign is sometimes said to be a different *handedness* or *helicity*. You will learn more about this in the context of high energy physics in the lectures on [Quantum Field Theory](#).

As we mentioned above, we have not yet included the spin of the electron. This is trivial: the discussion above is simply repeated twice, once for spin $|\uparrow\rangle$ and once for spin $|\downarrow\rangle$. The upshot is that the low-energy excitations of graphene are described by four massless Dirac fermions. One pair comes from the spin degeneracy of the electrons; the other from the existence of two Dirac points \mathbf{K} and \mathbf{K}' , sometimes referred to as the *valley degeneracy*.

4.2 Dynamics of Bloch Electrons

In this section, we look more closely at how electrons moving in a lattice environment react to external forces. We call these electrons *Bloch electrons*. We start by describing how some familiar quantities are redefined for Bloch electrons.

For simplicity, consider an insulator and throw in one further electron. This solitary electron sits all alone in an otherwise unoccupied band. The possible states available to it have energy $E(\mathbf{k})$ where \mathbf{k} lies in the first Brillouin zone. (The energy should also have a further discrete index which labels the particular band the electron is sitting in, but we'll suppress this in what follows). Despite its environment, we can still assign some standard properties to this electron.

4.2.1 Velocity

The average velocity \mathbf{v} of the electron is

$$\mathbf{v} = \frac{1}{\hbar} \frac{\partial E}{\partial \mathbf{k}} \quad (4.5)$$

First note that this is simply the *group velocity* of a wavepacket (a concept that we've met previously in the lectures on [Electromagnetism](#)). However, the “average velocity” means something specific in quantum mechanics, and to prove (4.5) we should directly compute $\mathbf{v} = \frac{1}{m} \langle \psi | -i\hbar \nabla | \psi \rangle$.

Bloch's theorem ensures that the electron eigenstates take the form

$$\psi_{\mathbf{k}}(\mathbf{x}) = e^{i\mathbf{k} \cdot \mathbf{x}} u_{\mathbf{k}}(\mathbf{x})$$

with \mathbf{k} in the Brillouin zone. As with the energy, we've suppressed the discrete band index on the wavefunction. The full wavefunction satisfies $H\psi_{\mathbf{k}}(\mathbf{x}) = E(\mathbf{k})\psi_{\mathbf{k}}(\mathbf{x})$, so that $u_{\mathbf{k}}(\mathbf{x})$ obeys

$$H_{\mathbf{k}} u_{\mathbf{k}}(\mathbf{x}) = E(\mathbf{k}) u_{\mathbf{k}}(\mathbf{x}) \quad \text{with} \quad H_{\mathbf{k}} = \frac{\hbar^2}{2m} (-i\nabla + \mathbf{k})^2 + V(\mathbf{x}) \quad (4.6)$$

We'll use a slick trick. Consider the Hamiltonian $H_{\mathbf{k}+\mathbf{q}}$ which we expand as

$$H_{\mathbf{k}+\mathbf{q}} = H_{\mathbf{k}} + \frac{\partial H_{\mathbf{k}}}{\partial \mathbf{k}} \cdot \mathbf{q} + \frac{1}{2} \frac{\partial^2 H_{\mathbf{k}}}{\partial k^i \partial k^j} q^i q^j \quad (4.7)$$

For small \mathbf{q} , we view this as a perturbation of $H_{\mathbf{k}}$. From our results of first order perturbation theory, we know that the shift of the energy eigenvalues is

$$\Delta E = \langle u_{\mathbf{k}} | \frac{\partial H_{\mathbf{k}}}{\partial \mathbf{k}} \cdot \mathbf{q} | u_{\mathbf{k}} \rangle$$

But we also know the exact result: it is simply $E(\mathbf{k} + \mathbf{q})$. Expanding this to first order in \mathbf{q} , we have the result

$$\langle u_{\mathbf{k}} | \frac{\partial H_{\mathbf{k}}}{\partial \mathbf{k}} | u_{\mathbf{k}} \rangle = \frac{\partial E}{\partial \mathbf{k}}$$

But this is exactly what we need. Using the expression (4.6) for $H_{\mathbf{k}}$, the left-hand side is

$$\frac{\hbar^2}{m} \langle u_{\mathbf{k}} | (-i\nabla + \mathbf{k}) | u_{\mathbf{k}} \rangle = \frac{\hbar}{m} \langle \psi_{\mathbf{k}} | -i\hbar\nabla | \psi_{\mathbf{k}} \rangle = \hbar \mathbf{v}$$

This gives our desired result (4.5).

It is perhaps surprising that eigenstates in a crystal have a fixed, average velocity. One might naively expect that the particle would collide with the crystal, bouncing all over the place with a corresponding vanishing average velocity. Yet the beauty of Bloch's theorem is that this is not what happens. The electrons can quite happily glide through the crystal structure.

A Filled Band Carries Neither Current nor Heat

Before we go on, we can use the above result to prove a simple result: a completely filled band does not contribute to the current. This is true whether the filled band is part of an insulator, or part of a metal. (In the latter case, there will also be a partially filled band which will contribute to the current.)

The current carried by each electron is $\mathbf{j} = -e\mathbf{v}$ where $-e$ is the electron charge. From (4.5), the total current of a filled band is then

$$\mathbf{j} = -\frac{2e}{\hbar} \int_{\text{BZ}} \frac{d^3k}{(2\pi)^3} \frac{\partial E}{\partial \mathbf{k}} \quad (4.8)$$

where the overall factor of 2 counts the spin degeneracy. This integral vanishes. This follows because $E(\mathbf{k})$ is a periodic function over the Brillouin zone and the total derivative of any periodic function always integrates to zero.

Alternatively, if the crystal has an *inversion symmetry* then there is a more direct proof. The energy satisfies $E(\mathbf{k}) = E(-\mathbf{k})$, which means that $\partial E(\mathbf{k})/\partial \mathbf{k} = -\partial E(-\mathbf{k})/\partial \mathbf{k}$ and the contributions to the integral cancel between the two halves of the Brillouin zone.

The same argument shows that a filled band cannot transport energy in the form of heat. The heat current is defined as

$$\mathbf{j}_E = 2 \int_{\text{BZ}} \frac{d^3k}{(2\pi)^3} E \mathbf{v} = \frac{1}{\hbar} \int_{\text{BZ}} \frac{d^3k}{(2\pi)^3} \frac{\partial(E^2)}{\partial \mathbf{k}}$$

which again vanishes when integrated over a filled band. This means that the electrons trapped in insulators can conduct neither electricity nor heat. Note, however, that while there is nothing else charged that can conduct electricity, there are other degrees of freedom – in particular, phonons – which can conduct heat.

4.2.2 The Effective Mass

We define the effective mass tensor to be

$$m_{ij}^* = \hbar^2 \left(\frac{\partial^2 E}{\partial k^i \partial k^j} \right)^{-1}$$

where we should view the right-hand side as the inverse of a matrix.

For simplicity, we will mostly consider isotropic systems, for which $m_{ij}^* = m^* \delta_{ij}$ and the effective mass of the electron is given by

$$m^* = \hbar^2 \left(\frac{\partial^2 E}{\partial k^2} \right)^{-1} \quad (4.9)$$

where the derivative is now taken in any direction. This definition reduces to something very familiar when the electron sits at the bottom of the band, where we can Taylor expand to find

$$E = E_{\min} + \frac{\hbar^2}{2m^*} |\mathbf{k} - \mathbf{k}_{\min}|^2 + \dots$$

This is the usual dispersion relation for a non-relativistic particle.

The effective mass m^* has more unusual properties higher up the band. For a typical band structure, m^* becomes infinite at some point in the middle, and is negative close to the top of the band. We'll see how to interpret this negative effective mass in Section 4.2.4.

In most materials, the effective mass m^* near the bottom of the band is somewhere between 0.01 and 10 times the actual mass of the electron. But there are exceptions. Near the Dirac point, graphene has an infinite effective mass by the definition (4.9), although this is more because we've used a non-relativistic definition of mass which is rather daft when applied to graphene. More pertinently, there are substances known, appropriately, as *heavy fermion materials* where the effective electron mass is around a 1000 times heavier than the actual mass.

A Microscopic View on the Effective Mass

We can get an explicit expression for the effective mass tensor m_{ij} in terms of the microscopic electron states. This follows by continuing the slick trick we used above, now thinking about the Hamiltonian (4.7) at second order in perturbation theory. This time, we find the inverse mass matrix is given by

$$(m^*)_{ij}^{-1} = \frac{\delta_{ij}}{m} + \frac{1}{m^2} \sum_{n \neq n'} \frac{\langle \psi_{n,\mathbf{k}} | p_i | \psi_{n',\mathbf{k}} \rangle \langle \psi_{n,\mathbf{k}} | p_j | \psi_{n',\mathbf{k}} \rangle - \text{h.c.}}{E_n(\mathbf{k}) - E_{n'}(\mathbf{k})}$$

where n labels the band of each state. Note that the second term takes the familiar form that arises in second order perturbation theory. We see that, microscopically, the additional contributions to the effective mass come from matrix elements between different bands. Nearby bands of a higher energy give a negative contribution to the effective mass; nearby bands of a lower energy give a positive contribution.

4.2.3 Semi-Classical Equation of Motion

Suppose now that we subject the electron to an external potential force of the form $\mathbf{F} = -\nabla U(\mathbf{x})$. The correct way to proceed is to add $U(\mathbf{x})$ to the Hamiltonian and solve again for the eigenstates. However, in many circumstances, we can work semi-classically. For this, we need that $U(\mathbf{x})$ is small enough that it does not distort the band structure and, moreover, does not vary greatly over distances comparable to the lattice spacing.

We continue to restrict attention to the electron lying in a single band. To proceed, we should think in terms of wavepackets, rather than plane waves. This means that the electron has some localised momentum \mathbf{k} and some localised position \mathbf{x} , within the bounds allowed by the Heisenberg uncertainty relation. We then treat this wavepacket as if it was a classical particle, where the position \mathbf{x} and momentum $\hbar\mathbf{k}$ depend on time. This is sometimes referred to as a *semi-classical* approach.

The total energy of this semi-classical particle is $E(\mathbf{k}) + U(\mathbf{x})$ where $E(\mathbf{k})$ is the band energy. The position and momentum evolve such that the total energy is conserved. This gives

$$\frac{d}{dt} \left(E(\mathbf{k}(t)) + U(\mathbf{x}(t)) \right) = \frac{\partial E}{\partial \mathbf{k}} \cdot \frac{d\mathbf{k}}{dt} + \nabla U \cdot \frac{d\mathbf{x}}{dt} = \mathbf{v} \cdot \left(\hbar \frac{d\mathbf{k}}{dt} + \nabla U \right) = 0$$

which is satisfied when

$$\hbar \frac{d\mathbf{k}}{dt} = -\nabla U = \mathbf{F} \quad (4.10)$$

This should be viewed as a variant of Newton's equation, now adapted to the lattice environment. In fact, we can make it look even more similar to Newton's equation. For an isotropic system, the effective "mass times acceleration" is

$$m^* \frac{d\mathbf{v}}{dt} = \frac{m^*}{\hbar} \frac{d}{dt} \left(\frac{\partial E}{\partial \mathbf{k}} \right) = \frac{m^*}{\hbar} \left(\frac{d\mathbf{k}}{dt} \cdot \frac{\partial}{\partial \mathbf{k}} \right) \frac{\partial E}{\partial \mathbf{k}} = \hbar \frac{d\mathbf{k}}{dt} = \mathbf{F} \quad (4.11)$$

where you might want to use index notation to convince yourself of the step in the middle where we lost the effective mass m^* . It's rather nice that, despite the complications of the lattice, we still get to use some old equations that we know and love. Of course, the key to this was really the definition (4.9) of what we mean by effective mass m^* .

An Example: Bloch Oscillations

Consider a Bloch electron, exposed to a constant electric field \mathcal{E} . The semi-classical equation of motion is

$$\hbar \dot{\mathbf{k}} = -e\mathcal{E} \quad \Rightarrow \quad k(t) = k(0) - \frac{e\mathcal{E}}{\hbar}t$$

So the crystal momentum \mathbf{k} increases linearly. At first glance, this is unsurprising. But it leads to a rather surprising effect. This is because \mathbf{k} is really periodic, valued in the Brillouin zone. Like a character in a 1980s video game, when the electron leaves one edge of the Brillouin zone, it reappears on the other side. 🧑

🧑 We can see what this means in terms of velocity. For a typical one-dimensional band structure shown on the right, the velocity $\mathbf{v} \sim \mathbf{k}$ in the middle of the band, but $\mathbf{v} \sim -\mathbf{k}$ as the particle approaches the edge of the Brillouin zone. In other words, a constant electric field gives rise to an oscillating velocity, and hence an oscillating current! This surprising effect is called *Bloch oscillations*.

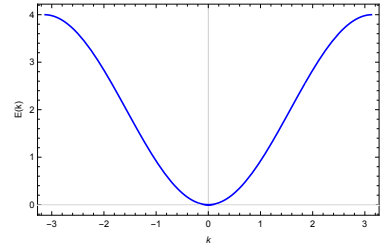


Figure 63:

As an example, consider a one-dimensional system with a tight-binding form of band structure

$$E = -C \cos(ka)$$

Then the velocity in a constant electric field oscillates as

$$v(k) = \frac{Ca}{\hbar} \sin(ka) = -\frac{Ca}{\hbar} \sin\left(\frac{e\mathcal{E}a}{\hbar}t\right)$$

The Bloch frequency is $\omega = e\mathcal{E}a/\hbar$. If we construct a wavepacket from several different energy eigenstates, then the position of the particle will similarly oscillate back and forth. This effect was first predicted by Leo Esaki in 1970.

Bloch oscillations are somewhat counterintuitive. They mean that a DC electric field applied to a pure crystal does *not* lead to a DC current! Yet we've all done experiments in school where we measure the DC current in a metal! This only arises because a metal is not a perfect crystal and the electrons are scattered by impurities or thermal lattice vibrations (phonons) which destroy the coherency of Bloch oscillations and lead to a current.

Bloch oscillations are delicate. The system must be extremely clean so that the particle does not collide with anything else over the time necessary to see the oscillations. This is too much to ask in solid state crystals. However, Bloch oscillations have been observed in other contexts, such as cold atoms in an artificial lattice. The time variation of the velocity of Caesium atoms in an optical lattice is shown in the figure⁸.

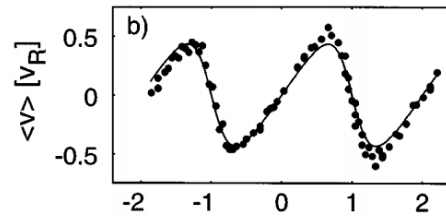


Figure 64:

4.2.4 Holes

Consider a totally filled band, and remove one electron. We're left with a vacancy in the otherwise filled band. In a zen-like manoeuvre, we ascribe properties to the absence of the particle. Indeed, as we will now see, this vacancy moves as if it were itself an independent particle. We call this particle a *hole*.

Recall that our definition (4.9) means that the effective mass of electrons is negative near the top of the band. Indeed, expanding around the maximum, the dispersion relation for electrons reads

$$E(\mathbf{k}) = E_{\max} + \frac{\hbar^2}{2m^*} |\mathbf{k} - \mathbf{k}_{\max}|^2 + \dots$$

and the negative effective mass $m^* < 0$ ensures that electrons have less energy as they move away from the maximum.

Now consider filling all states except one. As the hole moves away from the maximum, it costs more energy (because we're subtracting less energy!). This suggests that we should write the energy of the hole as

$$E_{\text{hole}}(\mathbf{k}) = -E(\mathbf{k}) = -E_{\max} + \frac{\hbar^2}{2m_{\text{hole}}^*} |\mathbf{k} - \mathbf{k}_{\max}|^2 + \dots$$

where

$$m_{\text{hole}}^* = -m^*$$

so that the effective mass of the hole is positive near the top of the band, but becomes negative if the hole makes it all the way down to the bottom.

⁸This data is taken from “*Bloch Oscillations of Atoms in an Optical Potential*” by Dahan et. al., Phys. Rev. Lett. vol 76 (1996), which reported the first observation of this effect.

The hole has other properties. Suppose that we take away an electron with momentum \mathbf{k} . Then the resulting hole can be thought of as having momentum $-\mathbf{k}$. This suggests that we define

$$\mathbf{k}_{\text{hole}} = -\mathbf{k} \quad (4.12)$$

However, the velocity of the hole is the same as that of the missing electron

$$\mathbf{v}_{\text{hole}} = \frac{1}{\hbar} \frac{\partial E_{\text{hole}}}{\partial \mathbf{k}_{\text{hole}}} = \frac{1}{\hbar} \frac{\partial E}{\partial \mathbf{k}} = \mathbf{v}$$

This too is intuitive, since the hole is moving in the same direction as the electron that we took away.

The definitions above mean that the hole obeys the Newtonian force law with

$$m_{\text{hole}}^* \frac{d\mathbf{v}_{\text{hole}}}{dt} = -\mathbf{F} = \mathbf{F}_{\text{hole}} \quad (4.13)$$

At first sight, this is surprising: the hole experiences an opposite force to the electron. But there's a very simple interpretation. The force that we typically wish to apply to our system is an electric field \mathcal{E} which, for an electron, gives rise to

$$\mathbf{F} = -e\mathcal{E}$$

The minus sign in (4.13) is simply telling us that the hole should be thought of as carrying charge $+e$, the opposite of the electron,

$$\mathbf{F}_{\text{hole}} = +e\mathcal{E}$$

We can also reach this same conclusion by computing the current. We saw in (4.8) that a fully filled band carries no current. This means that the current carried by a partially filled band is

$$\mathbf{j} = -2e \int_{\text{filled}} \frac{d^3k}{(2\pi)^3} \mathbf{v}(\mathbf{k}) = +2e \int_{\text{unfilled}} \frac{d^3k}{(2\pi)^3} \mathbf{v}(\mathbf{k})$$

The filled states are electrons carrying charge $-e$; the unfilled states are holes, carrying charge $+e$.

Finally, it's worth mentioning that the idea of holes in band structure provides a fairly decent analogy for anti-matter in high-energy physics. There too the electron has a positively charged cousin, now called the positron. In both cases, the two particles can come together and annihilate. In solids, this releases a few eV of energy, given by the gap between bands. In high-energy physics, this releases a million times more energy, given by the rest mass of the electron.

4.2.5 Drude Model Again

The essence of Bloch's theorem is that electrons can travel through perfect crystals unimpeded. And yet, in the real world, this does not happen. Even the best metals have a resistance, in which any current degrades and ultimately relaxes to zero. This happens because metals are not perfect crystals, and the electrons collide with impurities and vacancies, as well as thermally vibrations called phonons.

We can model these effects in our semi-classical description by working with the electron equation of motion called the *Drude model*

$$m^* \dot{\mathbf{v}} = -e\mathcal{E} - \frac{m^*}{\tau} \mathbf{v} \quad (4.14)$$

Here \mathcal{E} is the applied electric field and τ is the *scattering time*, which should be thought of as the average time between collisions.

We have already met the Drude model in the lectures on [Electromagnetism](#) when we tried to describe the conductivity in metals classically. We have now included the quantum effects of lattices and the Fermi surface yet, rather remarkably, the equation remains essentially unchanged. The only difference is that the effective mass m^* will depend on \mathbf{k} , and hence on \mathbf{v} , if the electron is not close to the minimum of the band.

In equilibrium, the velocity of the electron is

$$\mathbf{v} = -\frac{e\tau}{m^*} \mathcal{E} \quad (4.15)$$

The proportionality constant is called the *mobility*, $\mu = |e\tau/m^*|$. The total current density $\mathbf{j} = -en\mathbf{v}$ where n is the density of charge carriers. The equation (4.15) then becomes $\mathbf{j} = \sigma\mathcal{E}$ where σ is the conductivity,

$$\sigma = \frac{e^2\tau n}{m^*} \quad (4.16)$$

We also define the resistivity $\rho = 1/\sigma$. This is the same result that we found in our earlier classical analysis, except the mass m is replaced by the effective mass m^* .

There is, however, one crucial difference that the existence of the Fermi surface has introduced. When bands are mostly unfilled, it is best to think of the charge carriers in terms of negatively charged electrons, with positive effective mass m^* . But when bands are mostly filled, it is best to think of the charge carriers in terms of positively charged holes, also with positive mass m_{hole}^* . In this case, we should replace the Drude model (4.14) with the equivalent version for holes,

$$m_{\text{hole}}^* \dot{\mathbf{v}} = +e\mathcal{E} - \frac{m_{\text{hole}}^*}{\tau} \mathbf{v} \quad (4.17)$$

This means that certain materials can appear to have positive charge carriers, even though the only things actually moving are electrons. The different sign in the charge carrier doesn't show up in the conductivity (4.16), which depends on e^2 . To see it, we need to throw in an extra ingredient.

Hall Resistivity

The standard technique to measure the charge of a material is to apply a magnetic field \mathbf{B} . Classically, particles of opposite charges will bend in opposite directions, perpendicular to \mathbf{B} . In a material, this results in the classical *Hall effect*.

We will discuss the motion of Bloch electrons in a magnetic field in much more detail in Section 4.3. (And we will discuss the Hall effect in much much more detail in [other lectures](#).) Here, we simply want to show how this effect reveals the difference between electrons and holes. For electrons, we adapt the Drude model (4.14) by adding a Lorentz force,

$$m^* \dot{\mathbf{v}} = -e(\mathcal{E} + \mathbf{v} \times \mathbf{B}) - \frac{m^*}{\tau} \mathbf{v}$$

We once again look for equilibrium solutions with $\dot{\mathbf{v}} = 0$. Writing $\mathbf{j} = -ne\mathbf{v}$, we now must solve the vector equation

$$\frac{1}{ne} \mathbf{j} \times \mathbf{B} + \frac{m^*}{ne^2 \tau} \mathbf{j} = \mathcal{E}$$

The solution to this is

$$\mathcal{E} = \rho \mathbf{j}$$

where the resistivity ρ is now a 3×3 matrix. If we take $\mathbf{B} = (0, 0, B)$, then we have

$$\rho = \begin{pmatrix} \rho_{xx} & \rho_{xy} & 0 \\ -\rho_{xy} & \rho_{xx} & 0 \\ 0 & 0 & \rho_{xx} \end{pmatrix}$$

where the diagonal, *longitudinal resistivity* is $\rho_{xx} = 1/\sigma$ where σ is given in (4.16). The novelty is the off-diagonal, Hall resistivity

$$\rho_{xy} = \frac{B}{ne}$$

We often define the *Hall coefficient* R_H as

$$R_H = \frac{\rho_{xy}}{B} = \frac{1}{ne}$$

This, as promised, depends on the charge e . This means that if we were to repeat the above analysis for holes (4.17) rather than electrons, we would find a Hall coefficient which differs by a minus sign.

There are metals – such as beryllium and magnesium – whose Hall coefficient has the “wrong sign”. We drew the Fermi surface for beryllium in Section 4.1.1; it contains both electrons and holes. In this case, we should add to two contributions with opposite signs. It turns out that the holes are the dominant charge carrier.

4.3 Bloch Electrons in a Magnetic Field

In this section, we continue our study of Bloch electrons, but now subjected to an external magnetic field \mathbf{B} . (Note that what we call \mathbf{B} should really be called \mathbf{H} ; it is the magnetising field, after taking into account any bound currents.) Magnetic fields play a particularly important role in solids because, as we shall see, they allow us to map out the Fermi surface.

4.3.1 Semi-Classical Motion

We again use our semi-classical equation of motion (4.10) for the electron, now with the Lorentz force law

$$\hbar \frac{d\mathbf{k}}{dt} = -e\mathbf{v} \times \mathbf{B} \quad (4.18)$$

where the velocity and momentum are once again related by

$$\mathbf{v} = \frac{1}{\hbar} \frac{\partial E}{\partial \mathbf{k}} \quad (4.19)$$

From these two equations, we learn two facts. First, the component of \mathbf{k} parallel to \mathbf{B} is constant: $\frac{d}{dt}(\mathbf{k} \cdot \mathbf{B}) = 0$. Second, the electron traces out a path of constant energy in \mathbf{k} -space. This is because

$$\frac{dE}{dt} = \frac{\partial E}{\partial \mathbf{k}} \cdot \frac{\partial \mathbf{k}}{\partial t} = -e\mathbf{v} \cdot (\mathbf{v} \times \mathbf{B}) = 0$$

These two facts are sufficient for us to draw the orbit in k -space. The Fermi surface is, by definition, a surface of constant energy. The electrons orbit the surface, perpendicular to \mathbf{B} . It’s pictured on the right for a spherical Fermi surface, corresponding to free electrons.

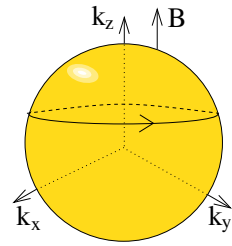


Figure 65:

Holes have an opposite electric charge, and so traverse the Fermi surface in the opposite direction. However, we have to also remember that we call \mathbf{k}_{hole} also has a relative minus sign (4.12). As an example, consider a metal with $Z = 2$, which has both electron and hole Fermi surfaces. In Figure 66, we have drawn the Fermi surfaces of holes (in purple) and electrons (in yellow) in the extended zone scheme, and shown their direction of propagation in a magnetic field.

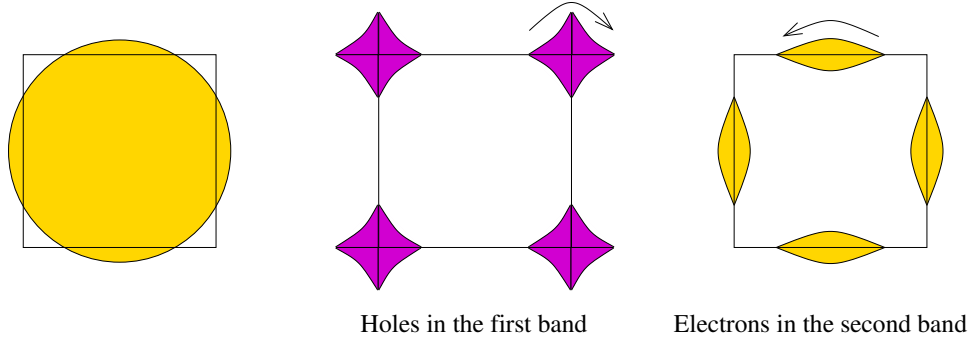


Figure 66: Pockets of electrons and holes for free electrons with $Z = 2$.

Orbits in Real Space

We can also look at the path $\mathbf{r}(t)$ that these orbits trace out in real space. Consider

$$\hat{\mathbf{B}} \times \hbar \dot{\mathbf{k}} = -e \hat{\mathbf{B}} \times (\dot{\mathbf{r}} \times \mathbf{B}) = -eB \dot{\mathbf{r}}_{\perp} \quad (4.20)$$

where \mathbf{r}_{\perp} is the position of the electron, projected onto a plane perpendicular to \mathbf{B} ,

$$\mathbf{r}_{\perp} = \mathbf{r} - (\hat{\mathbf{B}} \cdot \mathbf{r}) \hat{\mathbf{B}}$$

Integrating (4.20), we find

$$\mathbf{r}_{\perp}(t) = \mathbf{r}_{\perp}(0) - \frac{\hbar}{eB} \hat{\mathbf{B}} \times (\mathbf{k}(t) - \mathbf{k}(0)) \quad (4.21)$$

In other words, the particle follows the same shape trajectory as in \mathbf{k} -space, but rotated about \mathbf{B} and scaled by the magnetic length $l_B^2 = \hbar/eB$. For free electrons, with a spherical Fermi surface, this reproduces the classical result that electrons move in circles. However, as the Fermi surface becomes distorted by band effects this need no longer be the case, and the orbits in real space are no longer circles. For example, the electrons trace out the rosette-like shape in the $Z = 3$ Fermi surface that we saw in Figure 58. In extreme cases its possible for the real space orbits to not be closed curves at all. This happens, for example, if the Fermi surface is distorted more in one direction than another, so it looks like the picture on the right, with electrons performing a loop in the Brillouin zone. These are called *open Fermi surfaces*.

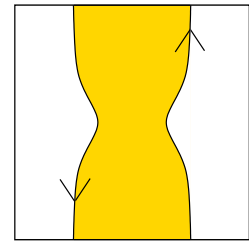


Figure 67:

4.3.2 Cyclotron Frequency

Let's compute the time taken for the electron to complete a closed orbit in \mathbf{k} -space. The time taken to travel between two points on the orbit $\mathbf{k}_1 = \mathbf{k}(t_1)$ and $\mathbf{k}_2 = \mathbf{k}(t_2)$ is given by the line integral

$$t_2 - t_1 = \int_{\mathbf{k}_1}^{\mathbf{k}_2} \frac{d\mathbf{k}}{|\dot{\mathbf{k}}|}$$

We can use (4.20) to relate $|\dot{\mathbf{k}}|$ to the perpendicular velocity,

$$|\dot{\mathbf{k}}| = \frac{eB}{\hbar} |\dot{\mathbf{r}}_{\perp}| = \frac{eB}{\hbar^2} \left| \left(\frac{\partial E}{\partial \mathbf{k}} \right)_{\perp} \right|$$

so we have

$$t_2 - t_1 = \frac{\hbar^2}{eB} \int_{\mathbf{k}_1}^{\mathbf{k}_2} \frac{d\mathbf{k}}{\left| \left(\frac{\partial E}{\partial \mathbf{k}} \right)_{\perp} \right|}$$

This has a rather nice geometric interpretation. Consider two orbits, both lying in the same plane perpendicular to \mathbf{B} , but with the second having a slightly higher Fermi energy $E + \Delta E$. To achieve this, the orbit must sit slightly outside the first, with momentum

$$\mathbf{k}' = \mathbf{k} + \left(\frac{\partial E}{\partial \mathbf{k}} \right)_{\perp} \Delta(k)$$

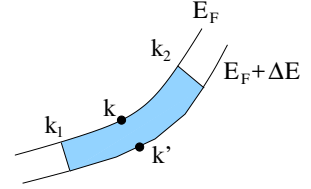


Figure 68:

where, as the notation suggests, $\Delta(\mathbf{k})$, can change as we move around the orbit. We require that $\Delta(\mathbf{k})$ is such that the second orbit also has constant energy,

$$\Delta E = \left| \left(\frac{\partial E}{\partial \mathbf{k}} \right)_{\perp} \right| \Delta(\mathbf{k})$$

The time taken to traverse the orbit can then be written as

$$t_2 - t_1 = \frac{\hbar^2}{eB} \frac{1}{\Delta E} \int_{\mathbf{k}_1}^{\mathbf{k}_2} \Delta(\mathbf{k}) d\mathbf{k}$$

But this is simply the area of the strip that separates the two orbits; this area, which we call A_{12} , is coloured in the figure. In the limit $\Delta E \rightarrow 0$, we have

$$t_2 - t_1 = \frac{\hbar^2}{eB} \frac{\partial A_{12}}{\partial E}$$

We can now apply this formula to compute the time taken to complete a closed orbit. Let $A(E)$ denote the area enclosed by the orbit. (Note that this will depend not only on E but also on the component of the momentum $\mathbf{k} \cdot \mathbf{B}$ parallel to the magnetic field.) The time taken to complete an orbit is

$$T = \frac{\hbar^2}{eB} \frac{\partial A(E)}{\partial E}$$

The *cyclotron frequency* is defined as

$$\omega_c = \frac{2\pi}{T} \tag{4.22}$$

One can check that the cyclotron frequency agrees with the usual result, $\omega_B = eB/m$ for free electrons.

The fact that the cyclotron frequency ω_c depends on some property of the Fermi surface – namely $\partial A/\partial E$ – is important because the cyclotron frequency is something that can be measured in experiments, since the electrons sit at resonance to absorb microwaves tuned to the same frequency. This gives us our first hint as to how we might measure properties of the Fermi surface.

4.3.3 Onsager-Bohr-Sommerfeld Quantisation

The combination of magnetic fields and Fermi surfaces gives rise to a host of further physics but to see this we will have to work a little harder.

The heart of the problem is that, in classical physics, the Lorentz force does no work. In the Hamiltonian formalism, this translates into the statement that the energy does not depend on \mathbf{B} when written in terms of the canonical momenta. Whenever the energetics of a system depend on the magnetic field, there must be some quantum mechanics going on underneath. In the present case, this means that we need to go slightly beyond the simple semi-classical description that we’ve met above, to find some of the discreteness that quantum mechanics introduces into the problem.

(As an aside: this problem is embodied in the Bohr-van-Leeuwen theorem, which states that there can be no classical magnetism. We describe how quantum mechanics can circumvent this in the discussion of Landau diamagnetism in the lectures on [Statistical Physics](#).)

To proceed, we would ideally like to quantise electrons in the presence of both a lattice and a magnetic field. This is hard. We’ve learned how to quantise in the presence of a magnetic field in Section 6 and in the presence of lattice in Section 3, but including both turns out to be a much more difficult problem. Nonetheless, as we now show, there’s a way to cobble together an approximation solution.

This cobbled-together quantisation was first proposed by Onsager, but follows an earlier pre-quantum quantisation of Bohr and Sommerfeld which suggests that, in any system, an approximation to the quantisation of energy levels can be found by setting

$$\frac{1}{2\pi} \oint \mathbf{p} \cdot d\mathbf{r} = \hbar(n + \gamma) \quad (4.23)$$

with $n \in \mathbf{Z}$ and γ an arbitrary constant. This Bohr-Sommerfeld quantisation does not, in general, agree with the exact result from solving the Schrödinger equation. However, it tends to capture the correct physics for large n , where the system goes over to its semi-classical description.

In the present context, we apply Bohr-Sommerfeld quantisation to our semi-classical model (4.18) and (4.19). We have

$$\frac{1}{2\pi} \oint \mathbf{p} \cdot d\mathbf{r} = \frac{\hbar}{2\pi} \oint \mathbf{k} \cdot d\mathbf{r} = \frac{\hbar^2}{2\pi eB} \oint \mathbf{k} \cdot (d\mathbf{k} \times \hat{\mathbf{B}})$$

where, in the last equality, we have used our result (4.20). But this integral simply captures the cross-sectional area of the orbit in k -space. This is the area $A(E)$ that we met above. We learn that the Bohr-Sommerfeld quantisation condition (4.23) leads to a quantisation of the cross-sectional areas of the Fermi surface in the presence of a magnetic field,

$$A_n = \frac{2\pi eB}{\hbar} (n + \gamma) \quad (4.24)$$

This quantisation of area is actually a variant of the Landau level quantisation that we met in Section 6.2. There are different ways of seeing this. First, note that, for fixed k_z , we can write the cyclotron frequency (4.22) as the difference between consecutive energy levels

$$\omega_c = \frac{2\pi eB}{\hbar^2} \frac{E_{n+1} - E_n}{A_{n+1} - A_n} = \frac{E_{n+1} - E_n}{\hbar}$$

Rearranging, this gives

$$E_n = \hbar\omega_c(n + \text{constant})$$

which coincides with our Landau level spectrum (6.14), except that the old cyclotron frequency $\omega_B = eB/m$ has been replaced by ω_c .

Alternatively, we could look at the quantisation of area in real space, rather than in \mathbf{k} -space. We saw in (4.21), that the orbit in real space has the same shape as that in \mathbf{k} -space, but is scaled by a factor of $l_B^2 = \hbar/eB$. This means that the flux through any such orbit is given by

$$\Phi_n = \left(\frac{\hbar}{eB} \right)^2 BA_n = (n + \gamma)\Phi_0 \quad (4.25)$$

where $\Phi_0 = 2\pi\hbar/e$ is the so-called *quantum of flux*. But this ties in nicely with our discussion in Section 6.2 of Landau levels in the absence of a lattice, where we saw that the degeneracy of states in each level is (6.17)

$$\mathcal{N} = \frac{\Phi}{\Phi_0}$$

which should clearly be an integer.

The quantisation (4.24) due to a background magnetic field results in a re-arrangement of the Fermi surface, which now sit in *Landau tubes* whose areas are quantised. A typical example is shown on the right.

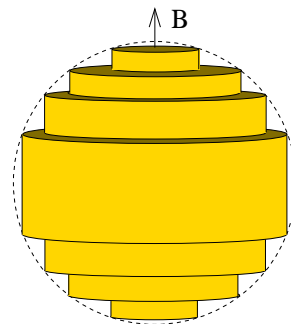


Figure 69:

4.3.4 Quantum Oscillations

The formation of Landau tubes gives rise to a number of fairly striking experimental signatures.

Consider a Fermi surface with energy E_F and a second surface slightly inside with energy $E_F - dE$. The region between these contains the accessible states if we probe the system with a small amount of energy dE . Now consider a Landau tube of cross-sectional area A_n , intersecting our Fermi surface. Typically, the Landau tube will intersect the Fermi surface only in some small region, as shown in left-hand picture of Figure 70. This means that the number of states that can contribute to physical processes will be fairly small. In the language that we introduced in the [Statistical Physics](#) lectures, the density of states $g(E_F)dE$ within this Landau tube will be small.

However, something special happens if the area A_n happens to coincide with an extremal area of the Fermi surface. Because the Fermi surface curves much more slowly at such points, the density of states $g(E_F)dE$ is greatly enhanced at this point. This is shown in the right-hand picture of Figure 70. In fact, one can show that the density of states actually diverges at this point as $g(E) \sim (E - E_*)^{-1/2}$.

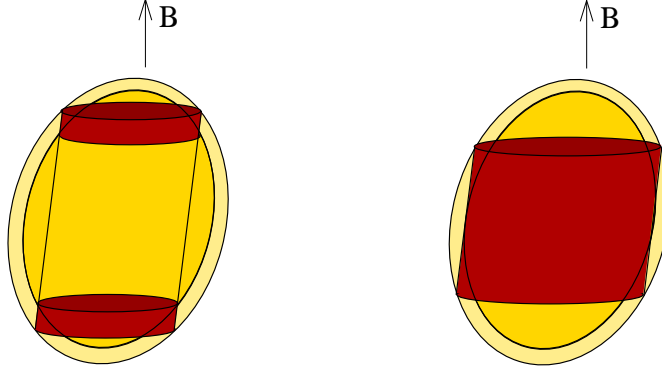


Figure 70: Landau tubes intersecting the Fermi surface: when the area of the tube coincides with an extremal cross-section of the Fermi surface, there is a large enhancement in the available states.

We learn that when the area quantisation takes special values, there are many more electrons that can contribute to any physical process. However, the area quantisation condition (4.24) changes with the magnetic field. This means that as we increase the magnetic field, the areas of Landau tubes will increase and will, occasionally, overlap with an extremal area in the Fermi surface. Indeed, if we denote the extremal cross-sectional area of the Fermi surface as A_{ext} , we must get an enhancement in the density of available states whenever

$$A_n = \frac{2\pi e B}{\hbar} (n + \gamma) = A_{\text{ext}}$$

for some n . We don't know what γ is, but this doesn't matter: the density of states should occur over and over again, at intervals given by

$$\Delta \left(\frac{1}{B} \right) = \frac{2\pi e}{\hbar} \frac{1}{A_{\text{ext}}}$$

Such oscillations are seen in a wide variety of physical measurements and go by the collective name of *quantum oscillations*.

The first, and most prominent example of quantum oscillation is the *de Haas-van Alphen effect*, in which the magnetisation $M = -\partial F / \partial B$ varies with magnetic field. The experimental data for gold is shown in the Figure⁹ 71. Note that there are two oscillation frequencies visible in the data. The Fermi surface of gold is shown on the

⁹The data is taken from I.M.Templeton, Proceedings of the Royal Society A, vol 292 (1965). Note the old school graph paper.

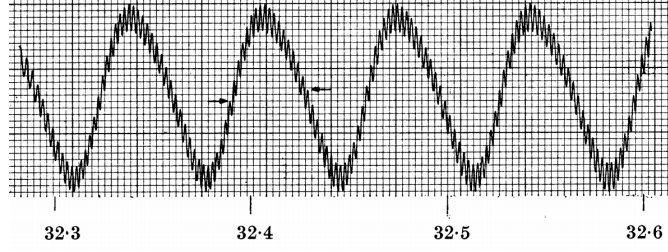


Figure 71: dHvA oscillations for gold. The horizontal axis is B , plotted in kG .

right. For the oscillations above, the magnetic field is parallel to the neck of the Fermi surface, as shown in the figure. The two frequencies then arise because there are two extremal cross-sections – the neck and the belly. As the direction of the magnetic field is changed, different extremal cross-sections become relevant. In this way, we can map out the entire Fermi surface.

The magnetisation is not the only quantity to exhibit oscillations. In fact, the large enhancement in the density of states affects nearly all observables. For example, oscillations in the conductivity are known as the *Shubnikov-de Haas effect*.

The experimental technique for measuring Fermi surfaces was pioneered by Brian Pippard, Cavendish professor and the first president of Clare Hall. Today, the techniques of quantum oscillations play an important role in attempts to better understand some of the more mysterious materials, such as unconventional superconductors.

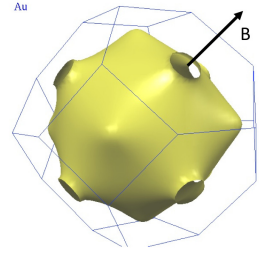


Figure 72: Gold